

## Searching for neutrino emission from the Cygnus region

Wenlian Li,<sup>a,\*</sup> Tian-Qi Huang,<sup>b,c</sup> Donglian Xu<sup>a,d</sup> and Huihai He<sup>b,c,e</sup> for the LHAASO collaboration

<sup>a</sup>*Tsung-Dao Lee Institute, Shanghai Jiao Tong University,  
201210 Shanghai, China*

<sup>b</sup>*Key Laboratory of Particle Astrophysics & Experimental Physics Division & Computing Center, Institute of High Energy Physics, Chinese Academy of Sciences,  
100049 Beijing, China*

<sup>c</sup>*Tianfu Cosmic Ray Research Center,  
610000 Chengdu, Sichuan, China*

<sup>d</sup>*School of Physics and Astronomy, Shanghai Jiao Tong University, Key Laboratory for Particle Astrophysics and Cosmology (MoE), Shanghai Key Laboratory for Particle Physics and Cosmology,  
200240 Shanghai, China*

<sup>e</sup>*University of Chinese Academy of Sciences,  
100049 Beijing, China*

*E-mail: [wenlianli@sjtu.edu.cn](mailto:wenlianli@sjtu.edu.cn), [huangtq@ihep.ac.cn](mailto:huangtq@ihep.ac.cn)*

The Cygnus region, which contains massive molecular and atomic clouds and young stars, is a promising Galactic neutrino source candidate. Cosmic rays transport in the region can produce neutrinos and  $\gamma$ -rays. Using ten years of track events detected by the IceCube Neutrino Observatory, we conduct searches for neutrino signals from the Cygnus region with a template method. Four templates, including the CO template, HI template, uniform template, and 2D Gaussian template, are used in this study. No significant emissions are found. We set upper limits for each template, with the resulting upper limit for the CO template being  $d\phi_\nu/dE_\nu = 6.25 \times 10^{-17} (E_\nu/100\text{TeV})^{-3} \text{TeV}^{-1} \text{cm}^{-2} \text{s}^{-1}$ .

38th International Cosmic Ray Conference (ICRC2023)  
26 July - 3 August, 2023  
Nagoya, Japan



\*Presenter

## 1. Introduction

The Cygnus region is an active star-forming area in our Galaxy and hosts various astrophysical sources, including massive young star clusters (YMCs, e.g., Cygnus OB2), pulsar wind nebulae (PWNe, e.g., TeV J2032+4130), and supernova remnants (SNRs, e.g.,  $\gamma$ -Cygni). Fermi-LAT has detected an excess of  $\gamma$ -ray emission from the Cygnus region over the interstellar background and all known sources, referred to as the Cygnus Cocoon [1]. This extended  $\gamma$ -ray source has also been observed at TeV energies by ARGO-YBJ [2] and HAWC [3]. The Large High Altitude Air Shower Observatory (LHAASO) also observed a 1.4 PeV photon from the direction of Cygnus OB2, suggesting the presence of a potential PeV cosmic-ray accelerator within the Cygnus region [4]. In such a scenario, the interactions between cosmic rays and the gas in the Cygnus region would lead to the production of diffuse neutrinos via deep inelastic collisions.

The IceCube Neutrino Observatory, located at the South Pole, is a cubic kilometer detector designed to detect neutrinos spanning from sub-TeV to 10 PeV [5]. IceCube has searched for neutrinos from the Cygnus region and constrained the hadronic component of  $\gamma$ -rays from this region to be less than 60% [6]. In this search, IceCube used eight years of track events from the northern sky, along with a neutrino emission template that assumes the neutrino flux is proportional to the observed  $\gamma$ -ray flux. However,  $\gamma$ -rays originating from known sources are not subtracted in this analysis, which could lead to a potential overestimation of the expected flux of diffuse neutrinos generated within this extended gas-rich region.

In this study, we conduct two analyses on the Cygnus region. Firstly, we search for neutrino emission from the Cygnus region with a template likelihood method. Four templates that describe the spatial distribution of neutrinos are used in this analysis. Secondly, we perform a scan of the Cygnus region and compare the obtained neutrino hot spots with the gas distribution and sources from the TeVcat [7]. All searches are performed using the ten-year muon-track data publicly released by IceCube [8].

## 2. Neutrino Data and Spatial Template

The public ten-year IceCube muon-track data consists of three components [8]: (i) experimental data events of each data sample; (ii) instrument response functions, which include the effective area  $A_{\text{eff}}(E_\nu, \delta_\nu)$  and the smearing matrix  $M(E_{\text{rec}}|E_\nu, \delta_\nu)$ ; and (iii) the detector uptime, which records the periods of data taking and enables the derivation of livetime for each data sample.

In this study, we test four different templates. Firstly, for the HI and CO templates, we assume that the neutrino flux is proportional to the gas column density  $N_{\text{HI}}$  [9] and  $N_{\text{CO}}$  [10] respectively, as neutrinos are produced through the hadronic interactions between cosmic rays and the interstellar medium. Next, we investigate a two-dimensional (2D) Gaussian template, as the Cygnus Cocoon is well described by a Gaussian profile with a width of  $\sim 2^\circ$  in the energy range from 10 TeV to 100 TeV [3]. The center of the 2D Gaussian template is located at the coordinates of the source LHAASO J2029+4036 ( $\alpha = 307.33^\circ$ ,  $\delta = 41.01^\circ$ ). Finally, we employ a uniform template, assuming that the spatial distribution of the neutrino flux is uniform within the region of interest (ROI), for comparison with the other templates. The uniform template is constructed as a circular area with a radius of  $10^\circ$ , centered at  $\alpha = 308.05^\circ$ ,  $\delta = 41.05^\circ$ , corresponding to the source LHAASO J2032+4102.

### 3. Searching for Neutrino Emission

An unbinned maximum likelihood method is widely used in the search for neutrino point sources [11, 12]. The general point source likelihood is defined as:

$$L(n_s, \gamma) = \prod_{i=1}^N \left( \frac{n_s}{N} S_i(\mathbf{x}_i, \sigma_i, E_i; \mathbf{x}_s, \gamma) + \left(1 - \frac{n_s}{N}\right) B_i(\sin\delta_i, E_i) \right) \quad (1)$$

where  $n_s$  is the number of signal events, and  $N$  is the total number of events.  $S_i$  is the signal probability density function (PDF), which is related to the location  $\mathbf{x}_i$ , angular uncertainty  $\sigma_i$ , and muon energy proxy  $E_i$  of the  $i$ th event, as well as the source location  $\mathbf{x}_s$  and the energy spectrum.  $B_i$  represents the background PDF estimated from data. Both signal and background likelihoods comprise spatial and energy PDFs. The signal spatial PDF is approximated as a 2D Gaussian with a width of  $\sigma_i$ , while the signal energy PDF is derived from the smearing matrix.

Considering the possibility of significant extended neutrino emission in the Cygnus region, as well as the morphology of neutrino emission may not follow a 2D Gaussian distribution, the point source likelihood is not suitable for the template search. Instead, we use the ps-template method developed by IceCube [13] to search for neutrino emission based on different templates. There are two key modifications compared to the point source likelihood. Firstly, a spatial template, rather than a 2D Gaussian function, is used to describe the spatial distribution of signal events. The ps-template method takes into account the source's extension by mapping the changing detector acceptance and convolving the template with the angular uncertainty of the events. Secondly, unlike the point source likelihood where the background is estimated using scrambled data with negligible contributions from point sources, for a large extended source, the signal events in the data must be subtracted. Therefore, we construct a signal-subtracted likelihood and estimate the background using scrambled data with the signal contamination subtracted [14]. The event-wise template likelihood is defined as

$$L(n_s, \gamma) = \prod_{i=1}^N \left( \frac{n_s}{N} S_i(\mathbf{x}_i, \sigma_i, E_i; \gamma) + \tilde{D}_i(\sin\delta_i, E_i) - \frac{n_s}{N} \tilde{S}_i(\sin\delta_i, E_i) \right) \quad (2)$$

where  $S_i$  denotes the signal PDF,  $\tilde{D}_i$  is the background PDF that is obtained from the scrambled data and thus contains the scrambled signal component, while  $\tilde{S}_i$  is the scrambled signal PDF.

The construction of the signal spatial PDF in the template likelihood can be described as follows:

$$S_i^{spat}(\mathbf{x}_i | \sigma_i, \gamma) = (T_{\text{spat}}(\mathbf{x}) \times M_{\text{acc}}(\mathbf{x}, \gamma) * \mathcal{G}_{2D}(\sigma_i))(\mathbf{x}_i) \quad (3)$$

We start with the spatial template  $T_{\text{spat}}$ , which is treated as the neutrino spatial template. By convolving it with IceCube acceptance  $M_{\text{acc}}$ , we can obtain the true neutrino direction after accounting for detector efficiency. Then this map is smoothed with a 2D Gaussian ( $\mathcal{G}_{2D}$ ) of width  $\sigma_i$  to account for the angular uncertainty of the event. Finally, this map is normalized to unity. The background PDF  $\tilde{D}_i$  is constructed as the same method in point source likelihood, while the scrambled signal PDF  $\tilde{S}_i$  is constructed following [15]. In the likelihood, we assume that neutrinos originating from the source follow a single power-law spectrum with spectral indices of  $\gamma = 2.5$  and  $\gamma = 3$ , respectively. The best-fit number of signal events  $\hat{n}_s$  is obtained by maximizing the template likelihood. The

test statistic (TS) is defined as the log-likelihood ratio between the maximized likelihood and the likelihood of background-only hypothesis, represented as  $TS = 2\ln(L(\hat{n}_s, \gamma)/L(n_s = 0))$ .

In addition to the template search, we conduct a scan of the Cygnus region using a  $20^\circ \times 20^\circ$  window to investigate the relationship between neutrinos and the gas distribution. The center of the scan region is located at the coordinates of LHAASO J2032+4102 ( $\alpha = 308.05^\circ$ ,  $\delta = 41.05^\circ$ ). The region is divided into a grid of points, each covering an area of  $0.1^\circ \times 0.1^\circ$ . For each grid point, we maximize the point source likelihood eq [1] to obtain the best-fit number of signal events  $\hat{n}_s$  and spectral index  $\hat{\gamma}$  under a power-law energy spectrum assumption. Furthermore, a local pretrial p-value is estimated for each point by conducting background trials. Each trial is obtained by scrambling the right ascension of each event in the data. While IceCube has performed an all-sky scan [16], our focus is specifically on the Cygnus region. By comparing the neutrino hot spots with the distribution of molecular clouds and HI gas, we aim to investigate a potential relationship between them.

#### 4. Summary and Discussion

Table 1 and Table 2 show the results of the template searches. In all templates, searches with a spectral index of  $\gamma = 3$  yield more significant results compared to  $\gamma = 2.5$ . The CO template with  $\gamma = 3$  yields the lowest pretrial p-value of 0.24, indicating the absence of a significant signal. Notably, the p-value obtained from the CO template is lower than that from the 2D Gaussian template, suggesting that the true spatial distribution of signals is more likely to resemble the former.

Spatial Template	$\gamma$	$\hat{n}_s$	Upper Limit $\phi_{90\%}$	Pretrial p-value
CO template	3	56.2	$6.25 \times 10^{-17}$	0.24
HI template	3	40.8	$6.69 \times 10^{-17}$	0.33
Uniform template	3	0.0	$5.80 \times 10^{-17}$	0.50
2D Gaussian template ( $\sigma = 2^\circ$ )	3	12.3	$3.04 \times 10^{-17}$	0.39

**Table 1:** Results of template searches. The spatial template, the spectral index  $\gamma$ , the best fit number of signal events  $\hat{n}_s$ , the 90% C.L. upper limit flux parameterized as  $d\phi_{\nu_\mu+\bar{\nu}_\mu}/dE_\nu = \phi_{90\%} \cdot (E_\nu/100 \text{ TeV})^{-\gamma} \text{TeV}^{-1} \text{cm}^{-2} \text{s}^{-1}$ , and the pretrial p-value of each search are listed.

Spatial Template	$\gamma$	$\hat{n}_s$	Upper Limit $\phi_{90\%}$	Pretrial p-value
CO template	2.5	27.3	$3.14 \times 10^{-16}$	0.34
HI template	2.5	12.5	$3.32 \times 10^{-16}$	0.44
Uniform template	2.5	0.0	$3.19 \times 10^{-16}$	0.50
2D Gaussian template ( $\sigma = 2^\circ$ )	2.5	5.0	$1.64 \times 10^{-16}$	0.45

**Table 2:** Results of template searches. Same as Table 1 but for  $\gamma = 2.5$ .

For the scan in the Cygnus region, Figure 1 shows the neutrino significance map along with the corresponding pretrial p-values. The neutrino significance map is compared to the distribution of molecular clouds (panel A) and HI gas (panel B). The contours representing the molecular cloud

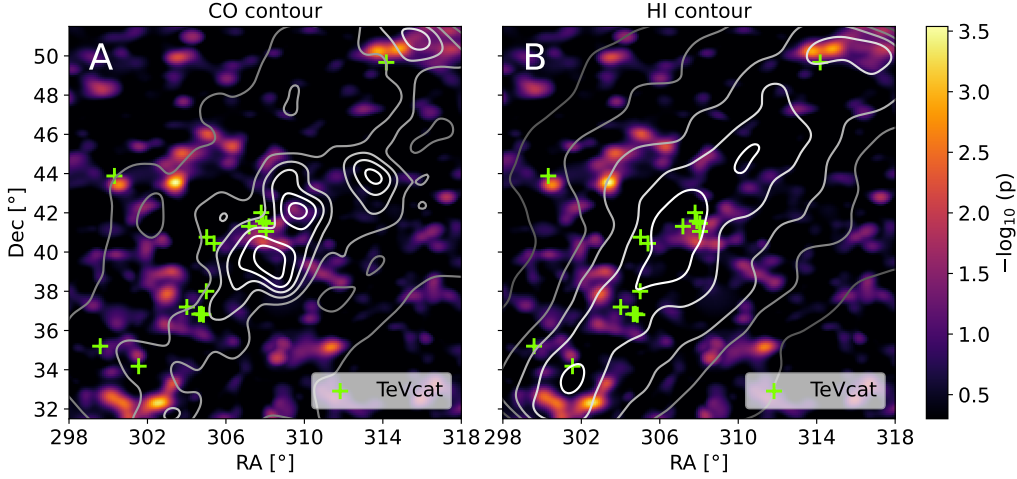


**Figure 1:** Neutrino significance skymap with pretrial p-value in the Cygnus region. The contours of the molecular cloud distribution (A) and HI gas distribution (B) are shown. TeVcat sources located in this region are indicated in green.

and HI gas distributions are smoothed using a Gaussian kernel with  $\sigma = 0.5^\circ$  to account for the angular uncertainty of the neutrino events.

In the Cygnus region, the most significant point is found at equatorial coordinates (J2000)  $\alpha = 303.4^\circ$ ,  $\delta = 43.5^\circ$  with a pretrial p-value of  $2.9 \times 10^{-4}$  ( $3.4\sigma$ ). At this point, the best fit parameters are  $\hat{n}_s = 20.1$  and  $\hat{\gamma} = 2.3$ . The most significant point is located  $4.22^\circ$  away from the center. Two  $\gamma$ -ray sources are located near the neutrino hot spots. One of them is the blazar MAGIC J2001+435 ( $\alpha = 300.32^\circ$ ,  $\delta = 43.88^\circ$ ), where neutrinos also exhibit a tendency to cluster ( $\alpha = 300.5^\circ$ ,  $\delta = 43.4^\circ$ ). IceCube previously reported the neutrino flux upper limit on this source MAGIC J2001+435 in the source-list searches using ten years of track data, with the pretrial p-value is found to be 0.21 ( $0.8\sigma$ ) [16]. The other source, RGB J2056+496 ( $\alpha = 314.18^\circ$ ,  $\delta = 49.67^\circ$ ), is situated near another neutrino hot spot ( $\alpha = 314.8^\circ$ ,  $\delta = 50.4^\circ$ ) where molecular clouds and HI gas are also present. In our search for neutrino emission from RGB J2056+496, we obtained a pretrial p-value of 0.07 ( $1.5\sigma$ ).

LHAASO is ideally located for observing the Cygnus region. With the accumulation of data, LHAASO will be able to accurately measure the diffuse  $\gamma$ -ray flux from the Cygnus region. This measurement will provide valuable information not only about the gas column density but also about the interaction rate of cosmic rays. In the future, we can conduct the template search using a brand new template based on the measurement of the diffuse  $\gamma$ -ray flux by LHAASO, which will offer a more comprehensive understanding of this complex region.

## References

- [1] M. Ackermann, M. Ajello, A. Allafort, L. Baldini, J. Ballet, G. Barbiellini et al., *A Cocoon of Freshly Accelerated Cosmic Rays Detected by Fermi in the Cygnus Superbubble*, *Science* **334** (2011) 1103.

- [2] B. Bartoli, P. Bernardini, X.J. Bi, P. Branchini, A. Budano, P. Camarri et al., *Identification of the TeV Gamma-Ray Source ARGO J2031+4157 with the Cygnus Cocoon*, *Astrophys. J.* **790** (2014) 152 [[1406.6436](#)].
- [3] A.U. Abeysekara, A. Albert, R. Alfaro, C. Alvarez, J.R.A. Camacho, J.C. Arteaga-Velázquez et al., *HAWC observations of the acceleration of very-high-energy cosmic rays in the Cygnus Cocoon*, *Nature Astronomy* **5** (2021) 465 [[2103.06820](#)].
- [4] Z. Cao, F.A. Aharonian, Q. An, L.X. Axikegu, Bai, Y.X. Bai, Y.W. Bao et al., *Ultrahigh-energy photons up to 1.4 petaelectronvolts from 12  $\gamma$ -ray Galactic sources*, *Nature* **594** (2021) 33.
- [5] ICECUBE collaboration, *The IceCube Neutrino Observatory: Instrumentation and Online Systems*, *JINST* **12** (2017) P03012 [[1612.05093](#)].
- [6] ICECUBE, HAWC collaboration, *IceCube Search for Galactic Neutrino Sources based on HAWC Observations of the Galactic Plane*, *PoS ICRC2019* (2020) 932 [[1908.08546](#)].
- [7] S.P. Wakely and D. Horan, *TeVcat: An online catalog for Very High Energy Gamma-Ray Astronomy*, in *International Cosmic Ray Conference*, vol. 3 of *International Cosmic Ray Conference*, pp. 1341–1344, Jan., 2008.
- [8] ICECUBE collaboration, *IceCube Data for Neutrino Point-Source Searches Years 2008-2018*, [2101.09836](#).
- [9] HI4PI Collaboration, N. Ben Bekhti, L. Flöer, R. Keller, J. Kerp, D. Lenz et al., *HI4PI: A full-sky HI survey based on EBHIS and GASS*, *Astron. Astrophys.* **594** (2016) A116 [[1610.06175](#)].
- [10] T.M. Dame, D. Hartmann and P. Thaddeus, *The Milky Way in Molecular Clouds: A New Complete CO Survey*, *Astrophys. J.* **547** (2001) 792 [[astro-ph/0009217](#)].
- [11] J. Braun, J. Dumm, F. De Palma, C. Finley, A. Karle and T. Montaruli, *Methods for point source analysis in high energy neutrino telescopes*, *Astroparticle Physics* **29** (2008) 299.
- [12] J. Braun, M. Baker, J. Dumm, C. Finley, A. Karle and T. Montaruli, *Time-dependent point source search methods in high energy neutrino astronomy*, *Astroparticle Physics* **33** (2010) 175.
- [13] ICECUBE collaboration, *Constraints on Galactic Neutrino Emission with Seven Years of IceCube Data*, *Astrophys. J.* **849** (2017) 67 [[1707.03416](#)].
- [14] ICECUBE collaboration, *Search for extended sources of neutrino emission with 7 years of IceCube data*, *PoS ICRC2017* (2018) 963.
- [15] E. Pinat, *The IceCube Neutrino Observatory: search for extended sources of neutrinos and preliminary study of a communication protocol for its future upgrade*, Ph.D. thesis, Brussels U., 2017.

- [16] ICECUBE collaboration, *Time-Integrated Neutrino Source Searches with 10 Years of IceCube Data*, *Phys. Rev. Lett.* **124** (2020) 051103 [1910.08488].

## Full Authors List: LHAASO Collaboration

Zhen Cao<sup>1,2,3</sup>, F. Aharonian<sup>4,5</sup>, Q. An<sup>6,7</sup>, Axikegu<sup>8</sup>, Y.X. Bai<sup>1,3</sup>, Y.W. Bao<sup>9</sup>, D. Bastieri<sup>10</sup>, X.J. Bi<sup>1,2,3</sup>, Y.J. Bi<sup>1,3</sup>, J.T. Cai<sup>10</sup>, Q. Cao<sup>11</sup>, W.Y. Cao<sup>7</sup>, Zhe Cao<sup>6,7</sup>, J. Chang<sup>12</sup>, J.F. Chang<sup>1,3,6</sup>, A.M. Chen<sup>13</sup>, E.S. Chen<sup>1,2,3</sup>, Liang Chen<sup>14</sup>, Lin Chen<sup>8</sup>, Long Chen<sup>8</sup>, M.J. Chen<sup>1,3</sup>, M.L. Chen<sup>1,3,6</sup>, Q.H. Chen<sup>8</sup>, S.H. Chen<sup>1,2,3</sup>, S.Z. Chen<sup>1,3</sup>, T.L. Chen<sup>15</sup>, Y. Chen<sup>9</sup>, N. Cheng<sup>1,3</sup>, Y.D. Cheng<sup>1,3</sup>, M.Y. Cui<sup>12</sup>, S.W. Cui<sup>11</sup>, X.H. Cui<sup>16</sup>, Y.D. Cui<sup>17</sup>, B.Z. Dai<sup>18</sup>, H.L. Dai<sup>1,3,6</sup>, Z.G. Dai<sup>7</sup>, Danzengluobu<sup>15</sup>, D. della Volpe<sup>19</sup>, X.Q. Dong<sup>1,2,3</sup>, K.K. Duan<sup>12</sup>, J.H. Fan<sup>10</sup>, Y.Z. Fan<sup>12</sup>, J. Fang<sup>18</sup>, K. Fang<sup>1,3</sup>, C.F. Feng<sup>20</sup>, L. Feng<sup>12</sup>, S.H. Feng<sup>1,3</sup>, X.T. Feng<sup>20</sup>, Y.L. Feng<sup>15</sup>, S. Gabici<sup>21</sup>, B. Gao<sup>1,3</sup>, C.D. Gao<sup>20</sup>, L.Q. Gao<sup>1,2,3</sup>, Q. Gao<sup>15</sup>, W. Gao<sup>1,3</sup>, W.K. Gao<sup>1,2,3</sup>, M.M. Ge<sup>18</sup>, L.S. Geng<sup>1,3</sup>, G. Giacinti<sup>13</sup>, G.H. Gong<sup>22</sup>, Q.B. Guo<sup>1,3</sup>, M.H. Gu<sup>1,3,6</sup>, F.L. Guo<sup>14</sup>, X.L. Guo<sup>8</sup>, Y.Q. Guo<sup>1,3</sup>, Y.Y. Guo<sup>12</sup>, Y.A. Han<sup>23</sup>, H.H. He<sup>1,2,3</sup>, H.N. He<sup>12</sup>, J.Y. He<sup>12</sup>, X.B. He<sup>17</sup>, Y. He<sup>8</sup>, M. Heller<sup>19</sup>, Y.K. Hor<sup>17</sup>, B.W. Hou<sup>1,2,3</sup>, C. Hou<sup>1,3</sup>, X. Hou<sup>24</sup>, H.B. Hu<sup>1,2,3</sup>, Q. Hu<sup>7,12</sup>, S.C. Hu<sup>1,2,3</sup>, D.H. Huang<sup>8</sup>, T.Q. Huang<sup>1,3</sup>, W.J. Huang<sup>17</sup>, X.T. Huang<sup>20</sup>, X.Y. Huang<sup>12</sup>, Y. Huang<sup>1,2,3</sup>, Z.C. Huang<sup>8</sup>, X.L. Ji<sup>1,3,6</sup>, H.Y. Jia<sup>8</sup>, K. Jia<sup>20</sup>, K. Jiang<sup>6,7</sup>, X.W. Jiang<sup>1,3</sup>, Z.J. Jiang<sup>18</sup>, M. Jin<sup>8</sup>, M.M. Kang<sup>25</sup>, T. Ke<sup>1,3</sup>, D. Kuleshov<sup>26</sup>, K. Kurinov<sup>26</sup>, B.B. Li<sup>11</sup>, Cheng Li<sup>6,7</sup>, Cong Li<sup>1,3</sup>, D. Li<sup>1,2,3</sup>, F. Li<sup>1,3,6</sup>, H.B. Li<sup>1,3</sup>, H.C. Li<sup>1,3</sup>, H.Y. Li<sup>7,12</sup>, J. Li<sup>7,12</sup>, Jian Li<sup>7</sup>, Jie Li<sup>1,3,6</sup>, K. Li<sup>1,3</sup>, W.L. Li<sup>20</sup>, W.L. Li<sup>13</sup>, X.R. Li<sup>1,3</sup>, Xin Li<sup>6,7</sup>, Y.Z. Li<sup>1,2,3</sup>, Zhe Li<sup>1,3</sup>, Zhuo Li<sup>27</sup>, E.W. Liang<sup>28</sup>, Y.F. Liang<sup>28</sup>, S.J. Lin<sup>17</sup>, B. Liu<sup>7</sup>, C. Liu<sup>1,3</sup>, D. Liu<sup>20</sup>, H. Liu<sup>8</sup>, H.D. Liu<sup>23</sup>, J. Liu<sup>1,3</sup>, J.L. Liu<sup>1,3</sup>, J.Y. Liu<sup>1,3</sup>, M.Y. Liu<sup>15</sup>, R.Y. Liu<sup>9</sup>, S.M. Liu<sup>8</sup>, W. Liu<sup>1,3</sup>, Y. Liu<sup>10</sup>, Y.N. Liu<sup>22</sup>, R. Lu<sup>18</sup>, Q. Luo<sup>17</sup>, H.K. Lv<sup>1,3</sup>, B.Q. Ma<sup>27</sup>, L.L. Ma<sup>1,3</sup>, X.H. Ma<sup>1,3</sup>, J.R. Mao<sup>24</sup>, Z. Min<sup>1,3</sup>, W. Mitthumsiri<sup>29</sup>, H.J. Mu<sup>23</sup>, Y.C. Nan<sup>1,3</sup>, A. Neronov<sup>21</sup>, Z.W. Ou<sup>17</sup>, B.Y. Pang<sup>8</sup>, P. Pattarakijwanich<sup>29</sup>, Z.Y. Pei<sup>10</sup>, M.Y. Qi<sup>1,3</sup>, Y.Q. Qi<sup>11</sup>, B.Q. Qiao<sup>1,3</sup>, J.J. Qin<sup>7</sup>, D. Ruffolo<sup>29</sup>, A. Sáiz<sup>29</sup>, D. Semikoz<sup>21</sup>, C.Y. Shao<sup>17</sup>, L. Shao<sup>11</sup>, O. Shchegolev<sup>26,30</sup>, X.D. Sheng<sup>1,3</sup>, F.W. Shu<sup>31</sup>, H.C. Song<sup>27</sup>, Yu.V. Stenkin<sup>26,30</sup>, V. Stepanov<sup>26</sup>, Y. Su<sup>12</sup>, Q.N. Sun<sup>8</sup>, X.N. Sun<sup>28</sup>, Z.B. Sun<sup>32</sup>, P.H.T. Tam<sup>17</sup>, Q.W. Tang<sup>31</sup>, Z.B. Tang<sup>6,7</sup>, W.W. Tian<sup>2,16</sup>, C. Wang<sup>32</sup>, C.B. Wang<sup>8</sup>, G.W. Wang<sup>7</sup>, H.G. Wang<sup>10</sup>, H.H. Wang<sup>17</sup>, J.C. Wang<sup>24</sup>, K. Wang<sup>9</sup>, L.P. Wang<sup>20</sup>, L.Y. Wang<sup>1,3</sup>, P.H. Wang<sup>8</sup>, R. Wang<sup>20</sup>, W. Wang<sup>17</sup>, X.G. Wang<sup>28</sup>, X.Y. Wang<sup>10</sup>, Y. Wang<sup>8</sup>, Y.D. Wang<sup>1,3</sup>, Y.J. Wang<sup>1,3</sup>, Z.H. Wang<sup>25</sup>, Z.X. Wang<sup>18</sup>, Zhen Wang<sup>13</sup>, Zheng Wang<sup>1,3,6</sup>, D.M. Wei<sup>12</sup>, J.J. Wei<sup>12</sup>, Y.J. Wei<sup>1,2,3</sup>, T. Wen<sup>18</sup>, C.Y. Wu<sup>1,3</sup>, H.R. Wu<sup>1,3</sup>, S. Wu<sup>1,3</sup>, X.F. Wu<sup>12</sup>, Y.S. Wu<sup>7</sup>, S.Q. Xi<sup>1,3</sup>, J. Xia<sup>7,12</sup>, J.J. Xia<sup>8</sup>, G.M. Xiang<sup>2,14</sup>, D.X. Xiao<sup>11</sup>, G. Xiao<sup>1,3</sup>, G.G. Xin<sup>1,3</sup>, Y.L. Xin<sup>8</sup>, Y. Xing<sup>14</sup>, Z. Xiong<sup>1,2,3</sup>, D.L. Xu<sup>13</sup>, R.F. Xu<sup>1,2,3</sup>, R.X. Xu<sup>27</sup>, W.L. Xu<sup>25</sup>, L. Xue<sup>20</sup>, D.H. Yan<sup>18</sup>, J.Z. Yan<sup>12</sup>, T. Yan<sup>1,3</sup>, C.W. Yang<sup>25</sup>, F. Yang<sup>11</sup>, F.F. Yang<sup>1,3,6</sup>, H.W. Yang<sup>17</sup>, J.Y. Yang<sup>17</sup>, L.L. Yang<sup>17</sup>, M.J. Yang<sup>1,3</sup>, R.Z. Yang<sup>7</sup>, S.B. Yang<sup>18</sup>, Y.H. Yao<sup>25</sup>, Z.G. Yao<sup>1,3</sup>, Y.M. Ye<sup>22</sup>, L.Q. Yin<sup>1,3</sup>, N. Yin<sup>20</sup>, X.H. You<sup>1,3</sup>, Z.Y. You<sup>1,3</sup>, Y.H. Yu<sup>7</sup>, Q. Yuan<sup>12</sup>, H. Yue<sup>1,2,3</sup>, H.D. Zeng<sup>12</sup>, T.X. Zeng<sup>1,3,6</sup>, W. Zeng<sup>18</sup>, M. Zha<sup>1,3</sup>, B.B. Zhang<sup>9</sup>, F. Zhang<sup>8</sup>, H.M. Zhang<sup>9</sup>, H.Y. Zhang<sup>1,3,6</sup>, J.L. Zhang<sup>16</sup>, L.X. Zhang<sup>10</sup>, Li Zhang<sup>18</sup>, P.F. Zhang<sup>18</sup>, P.P. Zhang<sup>7,12</sup>, R. Zhang<sup>7,12</sup>, S.B. Zhang<sup>2,16</sup>, S.R. Zhang<sup>11</sup>, S.S. Zhang<sup>1,3</sup>, X. Zhang<sup>9</sup>, X.P. Zhang<sup>1,3</sup>, Y.F. Zhang<sup>8</sup>, Yi Zhang<sup>1,12</sup>, Yong Zhang<sup>1,3</sup>, B. Zhao<sup>8</sup>, J. Zhao<sup>1,3</sup>, L. Zhao<sup>6,7</sup>, L.Z. Zhao<sup>11</sup>, S.P. Zhao<sup>12,20</sup>, F. Zheng<sup>32</sup>, B. Zhou<sup>1,3</sup>, H. Zhou<sup>13</sup>, J.N. Zhou<sup>14</sup>, M. Zhou<sup>31</sup>, P. Zhou<sup>9</sup>, R. Zhou<sup>25</sup>, X.X. Zhou<sup>8</sup>, C.G. Zhu<sup>20</sup>, F.R. Zhu<sup>8</sup>, H. Zhu<sup>16</sup>, K.J. Zhu<sup>1,2,3,6</sup> and X. Zuo<sup>1,3</sup>

<sup>1</sup>Key Laboratory of Particle Astrophysics & Experimental Physics Division & Computing Center, Institute of High Energy Physics, Chinese Academy of Sciences, 100049 Beijing, China. <sup>2</sup>University of Chinese Academy of Sciences, 100049 Beijing, China. <sup>3</sup>Tianfu Cosmic Ray Research Center, 610000 Chengdu, Sichuan, China. <sup>4</sup>Dublin Institute for Advanced Studies, 31 Fitzwilliam Place, 2 Dublin, Ireland. <sup>5</sup>Max-Planck-Institut für Nuclear Physics, P.O. Box 103980, 69029 Heidelberg, Germany. <sup>6</sup>State Key Laboratory of Particle Detection and Electronics, China. <sup>7</sup>University of Science and Technology of China, 230026 Hefei, Anhui, China. <sup>8</sup>School of Physical Science and Technology & School of Information Science and Technology, Southwest Jiaotong University, 610031 Chengdu, Sichuan, China. <sup>9</sup>School of Astronomy and Space Science, Nanjing University, 210023 Nanjing, Jiangsu, China. <sup>10</sup>Center for Astrophysics, Guangzhou University, 510006 Guangzhou, Guangdong, China. <sup>11</sup>Hebei Normal University, 050024 Shijiazhuang, Hebei, China. <sup>12</sup>Key Laboratory of Dark Matter and Space Astronomy & Key Laboratory of Radio Astronomy, Purple Mountain Observatory, Chinese Academy of Sciences, 210023 Nanjing, Jiangsu, China. <sup>13</sup>Tsung-Dao Lee Institute & School of Physics and Astronomy, Shanghai Jiao Tong University, 200240 Shanghai, China. <sup>14</sup>Key Laboratory for Research in Galaxies and Cosmology, Shanghai Astronomical Observatory, Chinese Academy of Sciences, 200030 Shanghai, China. <sup>15</sup>Key Laboratory of Cosmic Rays (Tibet University), Ministry of Education, 850000 Lhasa, Tibet, China. <sup>16</sup>National Astronomical Observatories, Chinese Academy of Sciences, 100101 Beijing, China. <sup>17</sup>School of Physics and Astronomy (Zhuhai) & School of Physics (Guangzhou) & Sino-French Institute of Nuclear Engineering and Technology (Zhuhai), Sun Yat-sen University, 519000 Zhuhai & 510275 Guangzhou, Guangdong, China. <sup>18</sup>School of Physics and Astronomy, Yunnan University, 650091 Kunming, Yunnan, China. <sup>19</sup>Département de Physique Nucléaire et Corpusculaire, Faculté de Sciences, Université de Genève, 24 Quai Ernest Ansermet, 1211 Geneva, Switzerland. <sup>20</sup>Institute of Frontier and Interdisciplinary Science, Shandong University, 266237 Qingdao, Shandong, China. <sup>21</sup>APC, Université Paris Cité, CNRS/IN2P3, CEA/IRFU, Observatoire de Paris, 119 75205 Paris, France. <sup>22</sup>Department of Engineering Physics, Tsinghua University, 100084 Beijing, China. <sup>23</sup>School of Physics and Microelectronics, Zhengzhou University, 450001 Zhengzhou, Henan, China. <sup>24</sup>Yunnan Observatories, Chinese Academy of Sciences, 650216 Kunming, Yunnan, China. <sup>25</sup>College of Physics, Sichuan University, 610065 Chengdu, Sichuan, China. <sup>26</sup>Institute for Nuclear Research of Russian Academy of Sciences, 117312 Moscow, Russia. <sup>27</sup>School of Physics, Peking University, 100871 Beijing, China. <sup>28</sup>School of Physical Science and Technology, Guangxi University, 530004 Nanning, Guangxi, China. <sup>29</sup>Department of Physics, Faculty of Science, Mahidol University, Bangkok 10400, Thailand. <sup>30</sup>Moscow Institute of Physics and Technology, 141700 Moscow, Russia. <sup>31</sup>Center for Relativistic Astrophysics and High

Energy Physics, School of Physics and Materials Science & Institute of Space Science and Technology, Nanchang University, 330031 Nanchang, Jiangxi, China. <sup>32</sup>National Space Science Center, Chinese Academy of Sciences, 100190 Beijing, China.

POS (ICRC2023) 1090